Optical properties of raindrops. Scattering into the forward hemisphere of observation under horizontal illumination

A.S. Glushchenko and V.V. Sterlyadkin

Moscow State Academy of Instrument Making and Information Science

Received August 4, 2004

Scattering properties of nonspherical raindrops are analyzed in geometric optics approximation. Mathematical simulation is performed for numerical models of shapes of the raindrops taking into account their oscillation during fall. Based on the simulation results, we propose an optimized geometrical scheme for optical disdrometer.

Interest in optical properties of raindrops is stimulated by the development of optical disdrometer for measurements of microstructure of precipitation. In traditional measurement schemes, one records amplitude of the pulse occurring due to shading of the direct light beam by a falling drop (Fig. 1*a*).

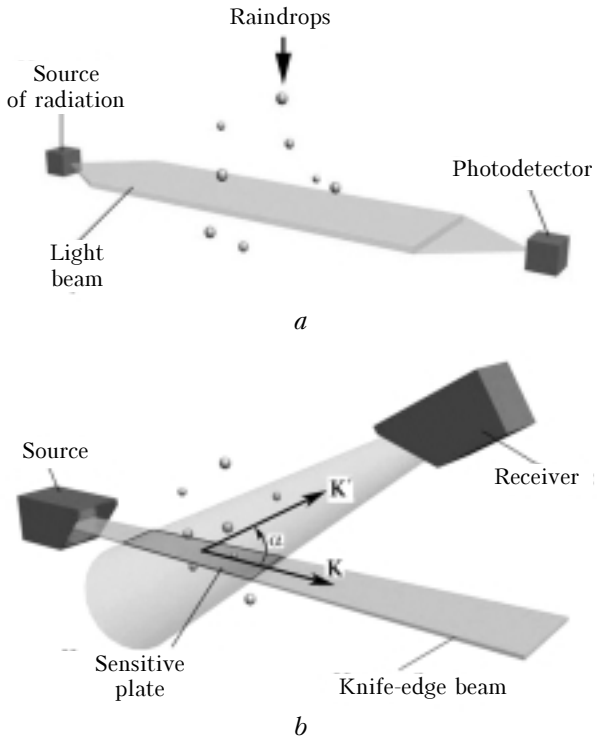

Fig. 1. Optical arrangement of a disdrometer, based on shading of direct beam (*a*) and on scattering at a sharp angle (*b*).

However, this method has a serious disadvantage because detector records total high-intensity flux directly from the source that produce high level of shot noise in the photodetector, against which it is very difficult to detect weak pulses due to shading. This is especially true when small droplets, less than 1 mm in diameter, are recorded.

In our opinion, a reasonable alternative to the method of shading of direct beam could be the method of measurements of optical pulses due to light scattering from drops into the forward hemisphere at sharp viewing angles (Fig. 1*b*). This method has no problems associated with the high level of shot noise of the photodetector, because it measures the optical signals from droplets at the level of dark current noise. Also, an advantage of this approach is that more than 90% of radiation is scattered by droplet into the forward hemisphere. A consequence is high sensitivity of the method and a possibility of measuring small particles and droplets. It is noteworthy, that traditional methods assume that (1) the amplitude of shadow-induced pulses is proportional to diameter D_{eff} of the effective spherical droplet when beam width is much less than the particle diameter, $h \ll D_{\text{eff}}$, and that (2) it is proportional to squared effective diameter D_{eff}^2 when beam width exceeds the effective diameter, $h > D_{\text{eff}}$. For nonspherical particles, D_{eff} is defined as a diameter of spherical droplet of the same volume. In both cases, the particle volume is calculated according to the amplitude of shading pulse.

Such methods of particle diameter determination can be considered absolutely valid under assumption that raindrops, falling into the beam, have stable shape uniquely related to the droplet volume, which is not actually true. Therefore, it is natural to consider the confidence of determination of a droplet volume and effective drop diameter, taking into account deformations of all types arising.

As known, raindrops during gravitational free fall in the atmosphere acquire oblate shape due to balance of aerodynamic air resistance, force of surface tension, internal hydrostatic pressure, as well as surface electrostatic charges, with stronger deformation occurring for larger droplets.[1] Such a deformation will be conventionally termed the static deformation of falling particles. In addition, our field

0235-6880/05/03 189-08 $02.00

measurements have proven that practically all (over 95%) of water droplets with effective diameter larger than 1 mm oscillate with the frequency of intrinsic capillary oscillations. The mean amplitude of such periodic oscillations $\Delta\gamma$ grows with increasing drop size nearly as quadratic law: $\Delta\gamma = AD^2$, where D is the droplet diameter; A is the coefficient, which depends on rainfall intensity and averages 0.006 mm^{-2} (see Ref. 2). This form of deformation will be called the deformation of a falling drop.

Taking into account the mean deformation and vibration, it becomes clear that drops with effective diameter 5 mm may have the shape factor $\gamma = 0.6$, and in this case the static deformation will be $\gamma = 0.75$, while the dynamic one due to amplitude of oscillations on the average will yield $\Delta\gamma = \pm 0.15$. It should be noted that in a number of recent foreign publications on the forward scattering by nonspherical droplets and determination of particle size from shading pulse, researchers take into account only static deformations, simultaneously assuming that the particle is static during fall.[3] However, even approximate calculations have shown that dynamical deformations additionally contribute to the error of drop size determination, with the magnitude of this contribution growing proportionally to the particle diameter.

In this regard, a natural question arises on how strongly do the deformations influence the accuracy of the optical methods of particle size measurements? The present paper is aimed at studying the optical properties of deformed raindrops to choose a disdrometer with an optical layout ensuring minimum effect of nonsphericity.

To achieve this task, it is necessary to calculate forward scattering phase functions of nonspherical water droplets for the range of angles $\alpha = 5 \ldots 90°$. Scattering angles less than 5° are of no practical interest owing to technical difficulty of measuring scattered radiation, as well as to strong diffraction effects on optical components of the transmitter. Angles in excess of 90° are not considered, because only very small fraction of radiation incident on the drop is scattered backwards, giving very weak backscattering signal.

For nonspherical particles, the scattering phase function will be a function of several variables, namely $I(\alpha, \beta, V, \gamma)$, where α and β are the viewing angles defining the direction of propagation of scattered radiation; γ is the drop shape factor; and V is the droplet volume. The shape of the oscillating drop to a good approximation can be represented as

$$\gamma = \gamma_{mean} + \Delta\gamma\cos(2\pi f), \qquad (1)$$

where γ_{mean} is the mean static deformation; $\Delta\gamma$ is the amplitude of droplet oscillation; and f is the frequency of intrinsic droplet oscillations. The deformation γ_{mean} depends on the droplet volume.

In calculations of the scattering phase functions, the static and dynamic deformations were taken into account. The static deformations were successfully studied by American scientists Beard and Chuang.[4] Based on laboratory experiments and calculations, they developed a numerical model of the shape of raindrops for a discrete set of particle diameters. We used this model as a basis in calculations for real raindrops. However, experiments of Beard and Chuang were performed in wind tunnels for separately flying drops, without the presence of turbulence, coagulation, and collisions of droplets with different sizes, i.e., without effects which in the natural precipitation lead to oscillation of droplet shape.

Numerous optical measurements of the falling drops in precipitation, performed by Sterlyadkin,[5] prove the existence of oscillations. The photographs of raindrops, presented by Schönhuber[6] and Chandrasekhar,[7] also indicate that instantaneous droplet shape substantially diverges from statistically averaged model by Beard and Chuang. Therefore, our calculations of the scattering phase functions were based on data on statistically average deformation γ_{mean} (supplemented with information on amplitude of oscillations $\Delta\gamma$, obtained by Sterlyadkin). Average deformation and amplitude of oscillations for falling drops are summarized in Table 1.

Table 1

D, mm	1	2	3	4	5
$\gamma_{mean}(D)$	0.97	0.942	0.89	0.78	0.72
$\Delta\gamma(D)$	0.007	0.028	0.063	0.112	0.1758

Thus, in the scattering phase function calculations we used as a final droplet model the sphere on which the static and dynamic deformations were superimposed. It was assumed that the drop has the static shape in accordance with Beard model, and experiences harmonic oscillations with amplitude $\Delta\gamma$. An example of graphic construction of this model, corresponding to different phases of oscillations for drop 5 mm in diameter, is shown in Fig. 2*a–c*. Figure 2*d–f* shows photographs of drops obtained by Schönhuber using fast-speed imaging of raindrops. It is easily seen that the analytical model well correlates with the shape of a real droplet.

In calculation of forward scattering phase functions, only first two derivative beams were taken into account. Their joint contribution to a given direction was about 99.5% of the total contribution of all beams. Such a high percentage is because, for all deformations considered, the third derivative beam, according to our calculations, did not fall into forward hemisphere; at the same time the contribution of the fourth derivative beam is very small, because every next reflection from droplet surface reduces the beam intensity by approximately an order of magnitude.

All geometrical considerations are based on right-handed Cartesian coordinate system. Rotation axis of a droplet was oriented along OZ-axis. Droplet surface was given in parametric form by

$$G(\phi, \psi, \gamma) = r(\psi)\begin{pmatrix} a(\gamma)\sin(\psi)\sin(\phi) \\ a(\gamma)\sin(\psi)\cos(\phi) \\ -c(\gamma)\cos(\psi) \end{pmatrix}, \qquad (2)$$

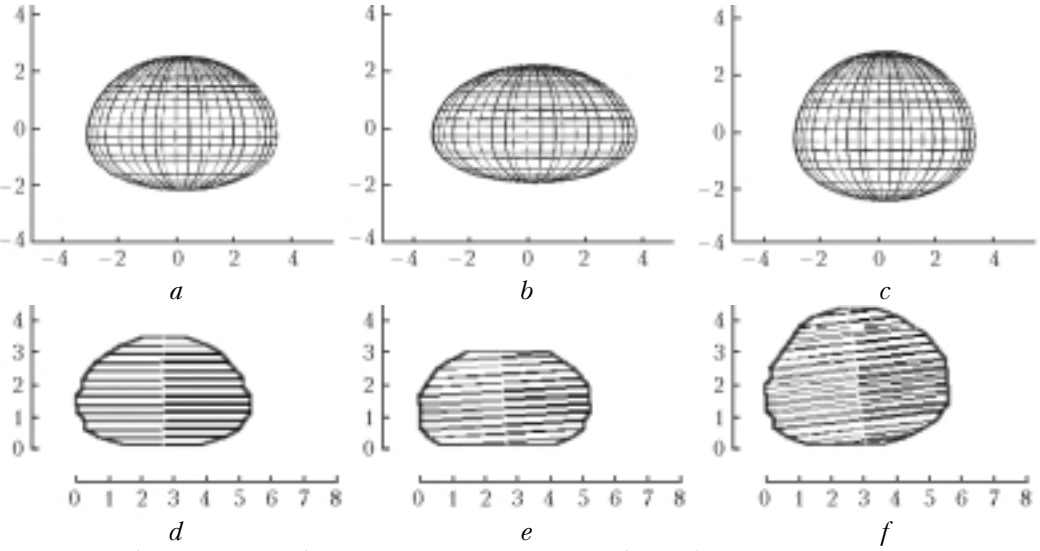

Fig. 2. Shapes of the drop with the diameter $D = 5$ mm, calculated for different oscillation phases: equilibrium (*a*); maximum oblate (*b*); maximum prolate (*c*); real raindrops with $D = 4.7$ mm in equilibrium, oblate, and prolate phases of oscillation[6] (*d*, *e*, *f*).

where $\phi = 0...2\pi$ is the azimuth measured from OY-axis clockwise; $\psi = 0...\pi$ is the angle of observation point counted off OZ-axis; $\gamma = c/a$ is the shape factor (c is vertical half-axis, and a is the horizontal half-axis of the ellipsoid of rotation); $r(\psi)$ is the additional factor function (which depends on the angle of observation point), required to describe the static deformation (for ellipsoid, $r(\psi) = 1$).

Expression in parentheses represents ellipsoid of rotation with vertical c and horizontal a half-axes. The static deformation is defined by the factor $r(\psi)$ and, in accordance with the Beard model, it is expressed as

$$r(\psi) = r_{\text{eff}}\left(1 + \sum_{m=0}^{10} c_m \cos(m\psi)\right), \qquad (3)$$

where r_{eff} is the effective radius of equal-volume spherical droplet; c_m are the numerical coefficients chosen for each effective spherical droplet diameter (Ref. 4, Table 2).

The droplet shape was calculated by substituting the coefficients of static deformation c_m (Table 2) and droplet shape factor γ into formula (2), with shape factor chosen in accordance with the calculated diameter using data from Table 1.

The calculation of the scattering phase function followed the traditional geometric-optics scheme. At the front of the incident wave, an infinitesimally small area dS_{inc} was formed, and then we calculated the trajectory of beams and incidence and reflection angles for each interaction of beams with droplet surface, and areas dS_1 and dS_2 on the observation sphere, corresponding to each beam exiting the drop; the radiative flux incident on each area was determined taking into account Fresnel coefficients.

The scattering phase functions were calculated for conditions of horizontal illumination of a droplet by plane wave and for two observation planes; a vertical plane passing through the droplet center, and a horizontal plane passing through the plane with maximum horizontal cross-sectional droplet area. During calculation, in each plane we specified N points on the droplet surface, upon which horizontal beams from source were incident, and which hereinafter will be called incidence points. For each of N incidence points, we calculated parameters of normal, angles of incidence and refraction, trajectories of beams inside the droplet, coordinates of points of interaction of beam with droplet surface, and trajectories of the beams exiting the droplet.

Following the terminology by Shifrin,[8] beams exiting the droplet will be called the derivative beams. The beam resulting from reflection of incident beam from droplet surface at the point of the first interaction (incidence point) is called the first derivative beam. The second derivative beam is the one suffering double refraction and exiting from the droplet at the point of second interaction. A geometric scheme of beams up to the second derivative beam inclusive for the incidence point, lying in the vertical plane, is presented in Fig. 3.

Table 2

Diameter D, mm	Shape factors $c_m \cdot 10000$, for different m										
	0	1	2	3	4	5	6	7	8	9	10
1	−28	−30	−83	−22	−3	2	1	0	0	0	0
2	−134	−118	−385	−100	−5	17	6	−1	−3	−1	1
3	−297	−247	−816	−188	24	52	13	−8	−8	−1	4
4	−481	−359	−1263	−244	91	99	15	−25	−16	2	10
5	−665	−435	−1674	−258	242	157	−7	−61	−21	11	17

The first-stage calculations yield a set of vectors $\mathbf{V}_i$, $i = (1...N)$, consisting of angles of incidence and refraction for points of interaction of beams with droplet surface, as well as viewing angles determining the directions of propagation for the first and second derivative beams:

$$\mathbf{V}_i = (\alpha_{\text{inc1}}, \alpha_{\text{refr1}}, \alpha_{\text{inc2}}, \alpha_{\text{refr2}}, \alpha_{\text{obs1}}, \beta_{\text{obs1}}, \alpha_{\text{obs2}}, \beta_{\text{obs2}}), \quad (4)$$

where α_{inc1} and α_{refr1} are the angles of incidence and refraction at the point of incidence; α_{inc2} and α_{refr2} are the angles of incidence and refraction at the second interaction point; α_{obs1}, β_{obs1}, α_{obs2}, and β_{obs2} are the viewing angles for the first and second derivative beams.

At the second stage, we calculated Fresnel coefficients. The calculated results were presented as sets of the vectors $\mathbf{F}_i$:

$$\mathbf{F}_i = (F_{p1}\ F_{s1}\ F_{p2}\ F_{s2}),\ i = (1...N). \quad (5)$$

The third stage involved the calculation of parameters of trajectories of shifted beams, resulting from shift of incidence point by infinitesimally small distance. The calculated results were presented in terms of vector $\mathbf{V}'_i$ with same elements as for vector $\mathbf{V}_i$ but for shifted beams:

$$\mathbf{V}'_i = (\alpha'_{\text{inc1}}, \alpha'_{\text{refr1}}, \alpha'_{\text{inc2}}, \alpha'_{\text{refr2}}, \alpha'_{\text{obs1}}, \beta'_{\text{obs1}}, \alpha'_{\text{obs2}}, \beta'_{\text{obs2}}),$$
$$i = (1...N). \quad (6)$$

Observation areas dS_1 and dS_2 for each ith incidence point were calculated taking into account that they are proportional to the product of the corresponding differences of viewing angles; the calculated results on these differences were also presented as separate vectors:

$$d\alpha_{\text{obs1},i} = \alpha_{\text{obs1},i} - \alpha'_{\text{obs1},i},\ \ d\beta_{\text{obs1},i} = \beta_{\text{obs1},i} - \beta'_{\text{obs1},i},$$

$$d\alpha_{\text{obs2},i} = \alpha_{\text{obs2},i} - \alpha'_{\text{obs2},i},\ \ d\beta_{\text{obs2},i} = \beta_{\text{obs2},i} - \beta'_{\text{obs2},i},$$

with $i = (1...N)$.

At the final stage, we calculated the discrete vectors of values of scattering phase functions for first two derivative beams $I1_i$, $I2_i$, $i = (1...N)$. For each i, there were the corresponding values of viewing angles for the first and second derivative beams. Then, the values of the scattering phase functions were linearly interpolated over viewing angles multiple of 5°. The total scattering phase function was calculated by the following formula:

$$I(\alpha_{\text{obs}}) = I1(\alpha_{\text{obs}}) + I2(\alpha_{\text{obs}}). \quad (7)$$

Since radiation, incident on the droplet, propagates in horizontal direction, the total radiative flux per droplet will be the product of intensity of light times cross-sectional area of droplet, perpendicular to the wave vector of the incident radiation. In calculations, we took as the initial parameters the position vector ρ and angle t. These quantities determine the coordinates of the point $A_{\text{pr}}(0, y_1, z_1)$, representing a projection of incidence point $A(x_1, y_1, z_1)$ onto the plane of vertical cross section of the droplet, namely YOZ-plane.

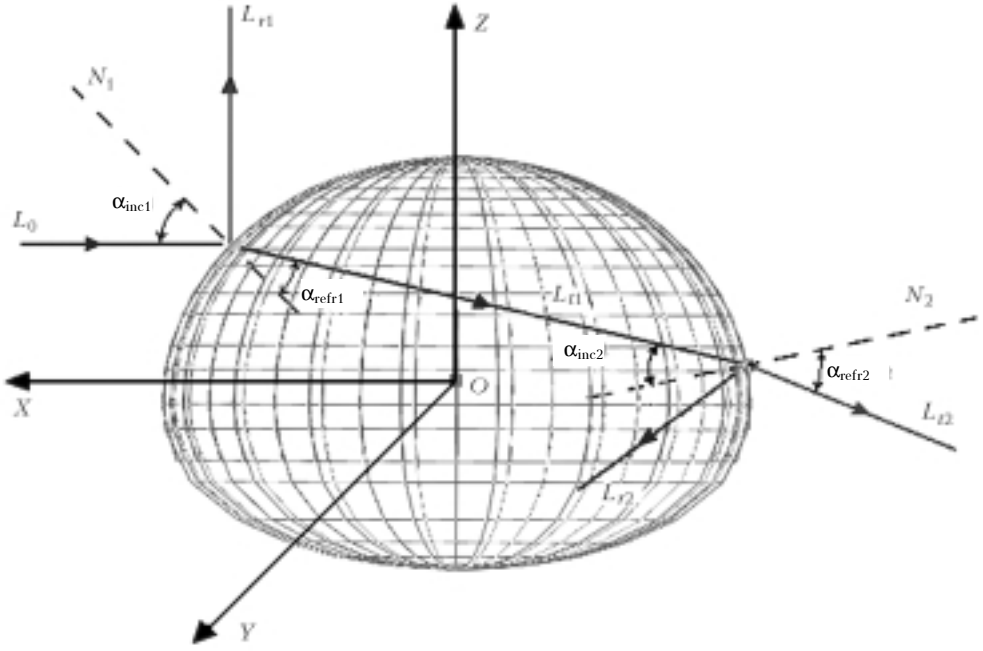

Fig. 3. Scheme of beam passage through a droplet: L_0 is the beam incident on droplet; N_1 is the normal at the incidence point; L_{r1} is the first derivative (reflected) beam; L_{t1} is the refracted beam at the incidence point; N_2 is the normal at the point of second interaction of the beam to the droplet surface; L_{r2} is the reflected beam at the second interaction point; L_{t2} is the second derivative (double refracted) beam.

According to the chosen parameters of the point A_{pr}, we calculated the coordinates of incidence point on the droplet surface A by solving the system of equations

$$\begin{cases} y_1 = \rho\cos(t), \\ z_1 = \rho\sin(t), \\ x_1 = G(\varphi_1,\psi_1,\gamma)_0, \\ y_1 = G(\varphi_1,\psi_1,\gamma)_1, \\ z_1 = G(\varphi_1,\psi_1,\gamma)_2. \end{cases} \quad (8)$$

With x_1, y_1, and z_1 determined in this way, the equation of the beam L_0, incident on the droplet, was written in the form of one-dimensional vector $(-p, y_1, z_1)$, where p is the parameter of a straight line. Then, we determined the spatial equation of normal to the droplet surface at the incidence point by solving the vector equation

$$\mathbf{N} = \left[\frac{\partial G(\varphi,\psi,\gamma)}{\partial\varphi}\ \frac{\partial G(\varphi,\psi,\gamma)}{\partial\psi}\right]. \quad (9)$$

Equation of normal, like the equation of incident beam, is a parametric function in the form of one-dimensional vector $\mathbf{N} = (a_{xn}p,\ a_{yn}p,\ a_{zn}p)$, where a_{xn}, a_{yn}, and a_{zn} are the angle-related parameters equivalent to direction cosines. From known equations of incident beam and normal, we determine the incidence angle at the point of the first interaction α_{inc}. Then, in accordance with Snell's law, we calculated the angle of refraction

$$n = \sin(\alpha_{inc})/\sin(\alpha_{refr}), \quad (10)$$

where n is the refractive index $n = n_2/n_1$; α_{inc} is the angle of beam incidence; α_{refr} is the angle of beam refraction; n_2 and n_1 are the refractive indices of the media inside and outside the droplet, respectively.

The refractive index of water depends on wavelength of optical radiation and varies from 1.328 to 1.343. In scattering phase function calculation it was assumed that $n = 4/3$.

For calculation of incident flux, at the front of incident beam an elemental area dS_{inc} was formed by incrementing two parameters: $t = t + dt$ and $\rho = \rho + d\rho$. At the same time, in the vertical cross section of droplet YOZ we obtain a shifted point A'_{pr}. For infinitesimally small $d\rho$ and dt, the corresponding area $dS_{inc} = \rho dt\, d\rho$.

The radiative flux per elemental areas dS_1 and dS_2 on the observation sphere is calculated taking into account their sizes in accordance with the following formulas:

$$dS_1 = R_{obs}\, d\alpha_1\, d\beta_1,\ dS_2 = R_{obs}\, d\alpha_2\, d\beta_2, \quad (11)$$

where R_{obs} is the radius of imaginary sphere of observation.

The quantities $d\alpha$ and $d\beta$ are increments of viewing angles, which were calculated based on trajectories of shifted and unshifted beams exiting the droplet according to the formulas:

$$d\alpha = \alpha - \alpha',\ d\beta = \beta - \beta'.$$

For each point of interaction of the beam with the droplet surface, we calculated the Fresnel coefficients. Taking into account the polarization, these coefficients were calculated as follows:

$$R_p = \frac{\tan^2(\alpha_{inc} - \alpha_{refr})}{\tan^2(\alpha_{inc} + \alpha_{refr})},\ R_s = \frac{\sin^2(\alpha_{inc} - \alpha_{refr})}{\sin^2(\alpha_{inc} + \alpha_{refr})}, \quad (12)$$

where R_s and R_p are the reflection coefficients for linearly polarized plane s and p waves, p wave is polarized in incidence plane; and s wave is polarized in the plane perpendicular to the incidence plane.

The directions of the beams exiting the droplets were determined with the help of viewing angles (α, β). The angle α lying in the vertical plane XOZ was measured from OX-axis and spanned the range $-\pi/2 < \alpha < \pi/2$. In turn, the angle β lying in horizontal plane XOY was measured from OX-axis and spanned the range $-\pi/2 < \beta < \pi/2$. Full variability ranges of α and β form the hemisphere of observation whose radius was assumed to be much more than the radius of droplet ($R_{obs} \gg r_{eff}$).

The scattering phase function was calculated by the following formula

$$I(\alpha,\ \beta) = \Delta W_{det}/\Delta\Omega, \quad (13)$$

where ΔW_{det} is the energy flux received by detector in the direction of scattering; and $\Delta\Omega$ is the solid angle on sphere of observation.

Formula for calculation of the solid angle is as follows:

$$\Delta\Omega = dS_{obs}/R^2_{obs}, \quad (14)$$

where dS_{obs} is the area illuminated on the sphere of observation.

The flux ΔW_{det} was calculated by the formula

$$\Delta W_{det} = \Delta W_{inc}\, K_{tr}, \quad (15)$$

where ΔW_{inc} is the flux incident on the receiving area dS_{inc}; K_{tr} is the transmission coefficient which accounts for interaction of the beam with the droplet surface. The scattering phase functions and transmission coefficients for first and second derivative beams K_1 and K_2 were calculated by the formulas:

$$I_1(\alpha_1,\beta_1) = \frac{I_0\rho dt\, d\rho K_1}{d\alpha_1\, d\beta_1},\ I_2(\alpha_2,\beta_2) = \frac{I_0\rho dt\, d\rho K_2}{d\alpha_2\, d\beta_2};$$

$$K_1 = \frac{1}{2}\left(R_{s1} + R_{p1}\right), \quad (16)$$

$$K_2 = \frac{1}{2}\left[(1 - R_{s1})(1 - R_{s2}) + \left(1 - R_{p1}\right)\left(1 - R_{p2}\right)\right],$$

where $I_0 = 1$, i.e., the intensity of wave incident on the droplet is assumed to be unity.

The total scattering phase function is calculated as follows

$$I(\alpha,\beta) = I_1(\alpha,\beta) + I_2(\alpha,\beta). \quad (17)$$

The scattering phase function was the function of a single variable. In calculation of the scattering

phase function for horizontal plane, the viewing angle $\alpha = 0$, while the scattering phase function had the dependence $I(\alpha_{obs}) = I(\beta)$, with $0 < \beta < \pi/2$. For vertical plane it was assumed that $\beta = 0$, $I(\alpha_{obs}) = I(\alpha)$ for $0 < \alpha < \pi/2$.

For ease of comparison of scattering phase functions for differently shaped droplets, we introduce the scattering function $J(\alpha,\beta,\gamma,D)$, normalized by droplet cross section according to the rule $J(\alpha,\beta,\gamma,D) = 4I(J(\alpha,\beta,\gamma,D))/\pi D^2$, where $D = 2r_{eff}$ is the effective droplet diameter.

The calculated results are given in terms of the plots of forward scattering phase function for spherical droplet, statically deformed droplet, and a maximum oblate oscillating droplet. Figure 4 shows three groups of dependences corresponding to horizontal and vertical planes of observation; and the latter results are additionally subdivided into those for upper and lower half planes in view of asymmetry of the vertical cross section of the droplet.

The calculated phase functions $J(\alpha,\gamma,D)$ of scattering into forward hemisphere of observation for statically deformed and maximum oblate droplets are summarized in Table 3. The $J(\alpha,\gamma,D)$ function is normalized by the cross-sectional area of a droplet of unit diameter.

In Fig. 4 the solid curve shows the scattering phase function of a spherical droplet γ_{sphere}, dashed line shows the scattering phase function of a maximum oblate droplet γ_{min}, and dots depict the scattering phase function of a statically deformed droplet γ_{st}. In Fig. 4*b*, in the region of 10° the three curves intersect, implying that the effect of deformations on the scattering properties of droplet should be minimum in this direction.

The radiative flux corresponding to the direction of scattering α_{obs} into the solid angle $d\Omega$ is calculated by the following formula

$$\Delta W_{det} = I_0 (\pi D^2/4) J(\gamma,\alpha,D) d\Omega.$$

The principle underlying the optical disdrometer measurements of microstructure of precipitation is the determination of sizes of individual falling droplets flying through a horizontal knife-edge beam. Particle size determination is performed by estimating the scattered radiative flux along a given viewing direction. The choice of the viewing direction is very critical; it directly determines the measured particle size range and the accuracy of particle size determination. To ensure the highest sensitivity of the instrument, it is desirable to choose such a direction for which the intensity of scattered radiation is close to maximum. From the plot of the scattering phase function of a spherical droplet (see Fig. 4) we can conclude that directions close to zero, i.e., region of forward scattering angles, is most favorable. On the other hand, directions close to 90°, for which values of scattering phase function decrease by two orders of magnitude, are to be considered useless for measurements because of too low signal level. Thus the range of considered viewing angles was 0–50°. At the same time, it should be taken into account that the calculations for small viewing angles (0–5°) neglected diffraction effects, quite significant for these angles. Therefore, in selecting optical arrangement of a disdrometer, the angles in the 0–5° range were not considered. Overall, the intensity of scattered radiation for angles less than 50° will decrease by no more than a factor of 8.

The static and dynamic deformations, characteristic of real raindrops, lead to a change of their scattering properties. The calculations of forward scattering phase functions showed that for some viewing directions these deformations have a significant influence, especially for large-diameter droplets. This distortion of the scattering phase function will be the source of additional error in determination of the drop sizes. Therefore, the second factor influencing the choice of viewing direction will be minimization of errors due to droplet deformation. To meet this requirement, it is necessary to find such scattering directions for which the intensity of radiation scattered by droplets is most stable for all considered drop sizes.

To achieve this, it is reasonable to analyze the maximum deviation $\Delta I(\alpha,\beta)$ of normalized scattering phase function of a deformed droplet $I'(\alpha,\beta)$ from scattering phase function of a relevant spherical droplet $I_0(\alpha,\beta)$:

$$\Delta I(\alpha,\beta) = \frac{I_0(\alpha,\beta) - I'(\alpha,\beta)}{I_0(\alpha,\beta)} \cdot 100. \qquad (18)$$

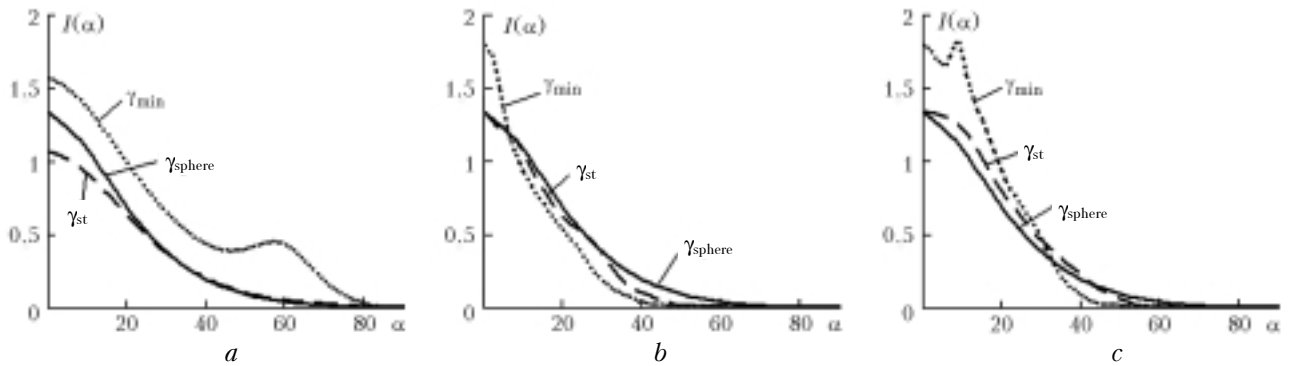

Fig. 4. Scattering phase functions of water droplets with the diameter of 5 mm: horizontal plane of observation (*a*); vertical plane, upper half plane of observation (*b*); vertical plane, lower half plane of observation (*c*).

Table 3

	α_{obs}, deg	Statically deformed droplet					Oscillating droplet in maximum oblateness phase				
		Effective droplet diameter $D = 2r$, mm									
		1	2	3	4	5	1	2	3	4	5
Horizontal plane of observation	0	1.173	1.158	1.147	1.104	1.116	1.166	1.141	1.119	1.117	1.064
	5	1.121	1.104	1.09	1.051	1.063	1.115	1.087	1.061	1.065	1.01
	10	1.007	0.99	0.972	0.941	0.954	1.002	0.974	0.946	0.958	0.905
	15	0.849	0.837	0.817	0.795	0.808	0.845	0.824	0.797	0.816	0.771
	20	0.678	0.671	0.653	0.639	0.652	0.675	0.661	0.641	0.663	0.627
	30	0.386	0.384	0.374	0.37	0.383	0.385	0.379	0.371	0.393	0.369
	40	0.199	0.198	0.194	0.194	0.206	0.198	0.196	0.194	0.213	0.199
	50	0.093	0.093	0.092	0.093	0.103	0.093	0.092	0.092	0.106	0.099
	60	0.041	0.042	0.041	0.043	0.049	0.041	0.04	0.039	0.046	0.048
	70	0.02	0.02	0.021	0.022	0.025	0.02	0.019	0.018	0.019	0.025
	80	0.0033	0.004	0.0043	0.0064	0.005	0.0032	0.0041	0.0046	0.0058	0.0054
	90	0.0022	0.0021	0.0019	0.0017	0.0014	0.0022	0.002	0.0018	0.0015	0.0014
Vertical plane, upper half plane of observation	0	1.2879	1.2998	1.3325	1.3617	1.3283	1.2835	1.287	1.326	1.4421	1.7868
	5	1.2246	1.2019	1.2227	1.2034	1.2117	1.222	1.1975	1.1981	1.2573	1.3448
	10	1.0855	1.0528	1.0948	1.0937	1.0437	1.0837	1.0569	1.079	1.0968	0.9212
	15	0.8991	0.8829	0.9467	0.9357	0.7969	0.899	0.8932	0.9318	0.862	0.7012
	20	0.7083	0.7156	0.7935	0.7546	0.6169	0.7097	0.7285	0.7687	0.6751	0.5259
	30	0.3952	0.4186	0.4834	0.4545	0.3604	0.3977	0.4299	0.4419	0.3492	0.1799
	40	0.2042	0.2077	0.2139	0.1656	0.0974	0.2058	0.2086	0.1711	0.0987	0.0357
	50	0.0955	0.0775	0.0686	0.0438	0.0103	0.0959	0.0697	0.0397	0.0116	0.014
	60	0.0422	0.0129	0.0062	0.0066	0.0071	0.0415	0.0055	0.0065	0.0076	0.0092
	70	0.0088	0.0037	0.0043	0.0048	0.0053	0.0056	0.0039	0.0045	0.0054	0.0059
	80	0.0027	0.0028	0.0033	0.0037	0.0038	0.0028	0.003	0.0034	0.004	0.0037
	90	0.0022	0.0023	0.0027	0.003	0.0027	0.0023	0.0025	0.0028	0.0029	0.0026
Vertical plane, lower half plane of observation	0	1.2879	1.2998	1.3325	1.3617	1.3283	1.2835	1.287	1.326	1.4421	1.7868
	5	1.2097	1.2359	1.2173	1.2722	1.3082	1.2066	1.2218	1.2467	1.3723	1.6608
	10	1.0536	1.0766	1.0301	1.0815	1.2134	1.0519	1.0666	1.0788	1.2287	1.6982
	15	0.8581	0.8807	0.826	0.8757	1.0074	0.8584	0.8757	0.8862	1.0072	1.2652
	20	0.664	0.6829	0.6307	0.6773	0.7869	0.6657	0.6812	0.6973	0.7939	0.9227
	30	0.3609	0.3718	0.3398	0.3637	0.4515	0.3633	0.3777	0.3866	0.4442	0.4556
	40	0.1829	0.1905	0.1706	0.1759	0.2222	0.1846	0.1939	0.1873	0.174	0.0806
	50	0.0851	0.0881	0.0691	0.0633	0.0585	0.0859	0.0866	0.0614	0.0239	0.0158
	60	0.0383	0.0386	0.0193	0.006	0.0064	0.0384	0.0309	0.0063	0.007	0.0072
	70	0.016	0.0047	0.0036	0.0035	0.0036	0.0125	0.0039	0.004	0.0039	0.0039
	80	0.0027	0.0028	0.0025	0.0023	0.0023	0.0027	0.0028	0.0027	0.0024	0.0023
	90	0.0022	0.0022	0.0018	0.0017	0.0017	0.0022	0.0022	0.0019	0.0017	0.0016

The calculated values of $\Delta J(\alpha,\beta)$ for nonspherical droplets are presented in Table 4; these are obtained taking into account the static and dynamic deformations for viewing angles in the range 5–50°. The calculations were performed for two planes of observation; and in the calculations for vertical plane the upper ($\alpha > 0$) and lower ($\alpha < 0$) half planes are considered separately.

From Table 4 it follows that the influence of deformation on scattering phase function was the least in the angular range $15 < \alpha < 35°$ in the vertical plane of observation in the upper half plane. It should be noted that the effect of nonsphericity for horizontal plane is also not very strong; however, for very oblate shapes ($\gamma \sim 0.85$) the scattering phase function is drastically distorted for scattering angles 40–60°.

The data presented in Table 4 are obtained in calculations of scattering phase functions of fixed-diameter droplets and the corresponding shape factors γ. The calculations showed that the deviation of scattering phase function of a deformed droplet from that of a spherical droplet is nonmonotonic. For instance, the static deformation leads to a decrease of scattering phase function for small viewing angles in the range 10–20°, consistent with the results obtained for ellipsoidal droplets. However, subsequent decrease of the coefficient γ causes increase of the scattering phase function for considered range of viewing angles, while the scattering phase function for maximum oblateness phase of droplet oscillations exceeds that of the spherical droplet. Therefore, it is impractical to use the optical arrangement of the disdrometric measurements of scattered radiation in the horizontal plane.

The calculations of scattering phase functions in the horizontal plane of observation demonstrated the presence of pronounced maxima in certain viewing directions, characteristic of most oblate droplets of

Table 4. Summary of maximum relative errors due to deformation $\Delta J(\alpha,\beta)$, %, for horizontal and vertical planes of observation

	D, mm	Viewing direction, deg									
		β									
Horizontal plane of observations		5	10	15	20	25	30	35	40	45	50
	1	3.42	3.00	0.90	1.70	3.60	4.60	5.00	4.89	4.60	3.78
	2	6.40	6.13	4.75	3.10	0.80	3.22	5.60	4.50	3.68	3.66
	3	14.10	13.50	10.20	5.60	1.80	1.10	4.20	4.80	5.20	5.80
	4	16.20	15.80	13.65	8.78	4.15	8.60	13.23	16.72	18.54	20.20
	5	23.41	28.90	33.60	39.90	44.32	57.56	82.00	> 100	> 100	> 100
		α									
Vertical plane of observations		5	10	15	20	25	30	35	40	45	50
	1	0.71	1.20	1.00	0.45	0.09	0.67	1.15	1.63	1.59	0.77
	2	4.40	4.90	2.88	1.24	5.00	6.90	5.40	1.02	14.80	37.60
	3	5.83	5.91	2.95	0.93	2.40	2.64	15.50	34.00	60.00	83.00
	4	9.47	13.20	11.52	10.64	9.24	18.30	39.00	57.40	78.00	91.00
	5	10.50	13.40	12.10	11.50	10.40	19.50	35.00	56.24	75.80	83.90
		α									
		−5	−10	−15	−20	−25	−30	−35	−40	−45	−50
	1	0.41	0.62	0.68	0.74	1.12	1.30	1.42	1.56	1.72	1.93
	2	3.90	4.20	5.32	6.50	7.20	8.90	10.53	12.50	13.80	11.80
	3	7.10	8.90	13.20	18.60	22.30	26.50	28.00	27.20	15.60	18.00
	4	17.10	21.20	22.50	24.00	29.80	35.00	38.65	25.00	20.80	29.50
	5	42.30	50.50	51.30	38.45	36.00	37.00	38.00	40.00	71.20	80.30

large diameters. The scattered intensity in directions of maxima may be more than a factor of two larger than the intensity of radiation scattered by the spherical droplet. The presence of this effect in the range of viewing angles considered here may seriously complicate the use of the method of radiation measurements in the horizontal plane.

Based on the calculations (Fig. 5), we suggested an optical arrangement of the disdrometric measurements of microstructure of precipitation, which, in our opinion, most successively minimizes the contribution from the particle deformations.

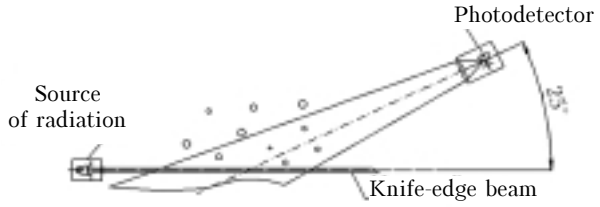

Fig. 5. Schematic illustration of the relative positions of source and optical detector in disdrometer measurements of microstructure of precipitation.

In the suggested scheme, raindrop of any diameter is expected to be measured with the accuracy within 3.4%.

References

1. K.V. Beard and C. Chuang, J. Atmos. Sci. **47**, No. 11, 1374–1389 (1990).
2. V.V. Sterlydkin, Atmos. Oceanic Opt. **13**, No. 5, 497–501 (2000).
3. B. Molle, in: *Int. Commission On Irrigation and Drainage.* Q. 50, R.3.02. Eighteen Congress, Montreal (2002).
4. K.V. Beard and C. Chuang, J. Atmos. Sci. **44**, No. 11, 1509–1524 (1987).
5. V.V. Sterlyadkin, Opt. Spektrosk. **69**, Issue 6, 1357–1392 (1990).
6. M. Schönhuber, *"About Interaction of Precipitation and Electromagnetic Waves,"* Doctoral Thesis, Technical University Graz, Austria (1998), 181 pp.
7. V. Chandrasekhar, A.C. William, and V.N. Bringi, J. Atmos. Sci. **45**, No. 8, 1323–1333 (1988).
8. K.S. Shifrin, *Light Scattering in Turbid Media* (Gostekhteorizdat, Leningrad, 1951), 288 pp.